Journal of Genetics and Genomics xxx (xxxx) xxx

Contents lists available at ScienceDirect

Journal of Genetics and Genomics

Journal homepage: www.journals.elsevier.com/journal-of-genetics-and-genomics/

Original Research

The OsCLV2s-OsCRN1 co-receptor regulates grain shape in rice

Xingxing Li [a, b, 1], Meng-en Wu [a, b, 1], Juncheng Zhang [a, b], Jingyue Xu [a, b], Yuanfei Diao [a, b], Yibo Li [a, b, *]

[a] National Key Laboratory of Crop Genetic Improvement and National Centre of Plant Gene Research (Wuhan), Huazhong Agricultural University, Wuhan, Hubei 430070, China
[b] Hubei Hongshan Laboratory, Wuhan, Hubei 430070, China

ARTICLE INFO

Article history:
Received 5 January 2024
Received in revised form
29 March 2024
Accepted 29 March 2024

Key words:
Rice
Grain shape
OsCLV2s
OsCRN1
Natural variations
Indica–*japonica* differentiation

ABSTRACT

The highly conserved CLV–WUS negative feedback pathway plays a decisive role in regulating stem cell maintenance in shoot and floral meristems in higher plants, including Arabidopsis, rice, maize, and tomato. Here, we report the discovery that *CLV*-like genes directly regulate grain shape in rice. We find significant natural variations in the *OsCLV2c*, *OsCLV2d*, and *OsCRN1* loci in a genome-wide association study of grain shape in rice. *OsCLV2a*, *OsCLV2c*, *OsCLV2d*, and *OsCRN1* negatively regulate grain length–width ratio and show distinctive geographical distribution, *indica*–*japonica* differentiation, and artificial selection signatures. Notably, OsCLV2a and OsCRN1 interact biochemically and genetically, suggesting that the two components function in a complex to regulate grain shape of rice. Furthermore, the genetic contributions of the haplotypes combining *OsCLV2a*, *OsCLV2c*, and *OsCRN1* are significantly higher than those of each single gene alone in controlling key yield traits. These findings identify two groups of receptor-like kinases that may function as distinct co-receptors to control grain size in rice, thereby revealing a previously unrecognized role of the *CLV* class genes in regulating seed development and proposing a framework to understand the molecular mechanisms of the CLV–WUS pathway in rice and other crops.

Introduction

Rice is one of the most important food crops worldwide feeding half of the world's population and also a model plant for fundamental research. Increasing rice yield is of great importance for supporting the rapid growth of the world population (Zhang, 2007; Harberd, 2015; Yu et al., 2022). The grain shape/size is highly heritable and one of the ideal models for studying organ shape development in higher plants and also determines the stable grain yield appearance and milling quality in rice (Zuo and Li, 2014; Zhang et al., 2021). A number of quantitative trait loci (QTL) or genes (QTGs) controlling rice grain shape by regulating cell division or cell expansion have been identified and are involved in several signaling pathways, including indole-3-acetic acid (IAA), cytokinin (CK), and brassinosteroids (BR) biosynthesis and signaling pathway, G protein signaling, mitogen-activated protein kinase (MAPK) signaling, the ubiquitin-proteasome degradation pathway, epigenetic pathways, peptide signaling, and transcriptional regulation (Fan and Li, 2019; Li et al., 2019). The genetic basis of grain size traits is very complex, as it is controlled by multiple QTGs (Ying et al., 2012); therefore, it remains to explore the functional QTGs and investigate their genetic relationship to understand the molecular mechanisms underlying genetic diversity (Fan and Li, 2019; Zhang et al., 2021).

Over the past decades, with the tremendous progress of molecular biology and next-generation sequencing (NGS) technologies, genome-wide association studies (GWAS) were available for the major cereal crop species to decipher the genetic basis of important agronomic traits for crop improvement (Purugganan and Jackson, 2021). Although some genes have been isolated using the map-based cloning approach, the position cloning method for QTL costs a lot of time and effort. In contrast, GWAS analysis benefits from high genetic diversity and a historical accumulation of recombination events, thus has the advantages of quickly identifying major genes for complex traits in diverse plants (Gupta et al., 2019). Although several high-quality genotype–phenotype associations have been identified in important crops (Tao et al., 2020; Liu et al., 2021a, Liu et al., 2022; Song et al., 2023), further efforts by taking full advantage of GWAS in rice are needed to discover relationship of

* Corresponding author.
E-mail address: liyibo@mail.hzau.edu.cn (Y. Li).
[1] These authors contributed equally to the work.

https://doi.org/10.1016/j.jgg.2024.03.011

Please cite this article as: X. Li, M.-e. Wu, J. Zhang *et al.*, The OsCLV2s-OsCRN1 co-receptor regulates grain shape in rice, Journal of Genetics and Genomics, https://doi.org/10.1016/j.jgg.2024.03.011

QTGs to close the gaps between genomic studies and practical breeding.

The shoot apical meristem (SAM) is governed by the CLAVATA (CLV)-WUSCHEL (WUS) negative feedback loop that the CLV3 peptide binds to the receptors of CLV1, CLV2/CORYNE (CRN), or BARELY ANY MERISTEM1/2 (BAM1/2) to repress the expression of *WUS*, which could promote the stem cell growth. On the contrary, the WUS transcription factor migrating from the organizing center to the central zone increases the transcription of *CLV3*, which could perfectly balance the proliferation and differentiation of stem cells and cooperatively ensure proper development (Somssich et al., 2016a; Kitagawa and Jackson, 2019; Hong and Fletcher, 2023). It is known that the broad function of the CLV−WUS pathway in controlling the meristem maintenance is conserved for agronomically important food crops. The mutants of *CLV* orthologs in maize showed an enlarged inflorescence meristem and fasciated ears (Fletcher, 2018). The weak alleles of *CLE* genes or *FASCIATED EAR3* (*FEA3*) maintain the meristem size, highlighting the potential to quantitatively manipulate *CLV* genes for yield enhancement (Bommert et al., 2013; Je et al., 2016; Liu et al., 2021b). In rice, although several components of the CLV−WUS pathway restricting stem cell accumulation specifically in floral or vegetative meristems were identified (Hong and Fletcher, 2023), the elaborate mechanism for regulating grain size in rice remains unknown.

It is reported that CRN and CLV2 act together to perceive the CLV3 signal, which is in parallel with CLV1 (Müller et al., 2008). In addition, CLV2 interacts with CRN via their transmembrane domains, and CRN mediates the localization of CLV2/CRN complexes to the plasma membrane (Bleckmann et al., 2010; Meng and Feldman, 2010; Zhu et al., 2010). CLV2/CRN may form multimers clustering in membrane subdomains with CLV1 or RECEPTOR-LIKE PROTEIN KINASE 2 (RPK2) (Zhu et al., 2010; Shinohara and Matsubayashi, 2015), but the genetic evidence suggests that the CLV2/CRN complex is functionally differentiated from the CLV1 and RPK2 complexes in plants (Nimchuk, 2017). The recent study revealed that CLAVATA3 INSENSITIVE RECEPTOR KINASES (CIKs) with short extracellular domains, which function as coreceptors of the CLV1, RPK2, and CLV2/CRN (Wang et al., 2022). Therefore, the further molecular mechanism in the CLV−WUS pathway needs to be characterized.

Despite that the important components of the CLV−WUS negative feedback loop are conserved in shoot, flower, and fruit development of Arabidopsis, rice, maize, and tomato (Xu et al., 2015; Fletcher, 2018), the function of OsCLV2 and OsCRN1 in regulating grain size in rice remains elusive. Here we provide natural variations of OsCLV2s and OsCRN1 for grain shape, which have distinctive geographical distribution, *indica*−*japonica* differentiation, and artificial selection signatures. The results act as evidence to explore the function of the conserved CLV−WUS signaling pathway in rice.

Results

OsCLV2c and *OsCLV2d* for grain shape contribute to *indica*−*japonica* differentiation

To identify genes for grain shape in rice, GWAS was conducted using grain length−width ratio as an indicator phenotype of the mini-core collection of 533 accessions worldwide (Table S1). A significant QTL on chromosome 6 was identified (Fig. 1A). Eleven possible candidate genes were identified after eliminating some transposons and retrotransposons around the peak of the QTL (Fig. 1B). The gene *LOC_Os06g38930* (IX, *OsCLV2c*) was supposed to be the candidate gene supported by the predominant expression pattern in 4-cm panicles (Fig. 1C; Table S2). To further explore the natural variations of *OsCLV2c*, we performed in-depth haplotype and geographical distribution analysis using the primary haplotypes in 4726 accessions worldwide (Wang et al., 2020; Zhao et al., 2021). Nine representative variations in the promoter and coding region of *OsCLV2c* were identified and classified into 9 haplotypes (H1−H9), and 2 major haplotypes H1 with 2080 accessions and H6 with 1089 accessions were identified (Fig. 1D; Table S3). There are significant differences between H1 and H6 in grain length−width ratio, grain length, panicle length, seeding height, and 1000-grain weight (Fig. 1E). The grain size trends of the two major haplotypes negatively co-related with the expression levels of *OsCLV2c* in 4-cm panicles, suggesting that *OsCLV2c* may negatively regulate the grain length−width ratio in rice (Fig. 1E). Coincidentally, the haplotype network analysis of *OsCLV2c* using the representative variations in the rice 4726 accessions suggested that *OsCLV2c* may contribute to *indica*−*japonica* differentiation (Fig. S1). In addition, the two major haplotypes of H1 and H6 had absolute advantages in the *indica* (92%) and *japonica* (94%) subspecies, respectively (Fig. 1F), indicating that *OsCLV2c* contributes greatly to *indica*−*japonica* differentiation. Subsequently, the geographical distribution of H1 and H6 showed that H1 was mainly found in Southeast Asia, while H6 was predominantly found in the Americas, Europe, and East Asia (Fig. 1G), inferring that the main haplotypes of *OsCLV2c* show obvious geographical distribution differentiation.

Coincidentally, the gene *LOC_Os06g38670* (II, *OsCLV2d*) homologous to *OsCLV2c* was also located in the peak locus (Fig. 1B), although its expression is moderate in 4-cm panicles (Fig. 1C; Table S2). Moreover, the expressions of *OsCLV2c* and *OsCLV2d* are predominant or specific in panicles, respectively, eliminating the *LOC_Os06g38750* (V) gene with high and specific expression in roots (Fig. S2), showing that *OsCLV2d* may also control grain shape in rice. Furthermore, haplotype analysis of *OsCLV2d* using 4726 accessions identified two major haplotypes of H1 ($n = 1396$) and H2 ($n = 1137$) among the 8 haplotypes determined by 13 major representative variations (Fig. 2A; Table S4). The lower length-width ratio, shorter and wider grains co-related to its higher expression in H2 than those in H1, suggesting that *OsCLV2d* may negatively regulate grain length−width ratio in rice (Fig. 2B). The haplotype cluster analysis of *OsCLV2d* among the 4726 accessions suggested *OsCLV2d* may contribute to *indica*−*japonica* differentiation (Fig. S3). Moreover, two major haplotypes H1 and H2 of *OsCLV2d* existed in the *indica* (90%) and *japonica* (88%) subspecies, respectively (Fig. 2C), hitting that *OsCLV2d* also confers the *indica*−*japonica* differentiation. In addition, H1 is largely found in Southeast Asian and North American countries; while H2 is mainly found in Southern Europe and East Asia (Fig. 2D), implying that the H1 and H2 of *OsCLV2d* possess the significant differentiation of geographical distribution in rice.

It could be speculated that *OsCLV2d* and *OsCLV2c*, clustered in one locus, function as a whole to control grain shape in rice. To confirm the genetic function of *OsCLV2c* and *OsCLV2d* in regulating grain size, we obtained the double mutant lines of *OsCLV2c* and *OsCLV2d* by using the CRISPR-Cas9 system in Zhonghua11 variety (ZH11) with the strong function haplotype of both alleles. The positive double mutant lines with different frameshift mutations exhibited longer and narrower grain shape than those of the wild type (Figs. 2E and S4), confirming that *OsCLV2c* and *OsCLV2d* negatively regulate grain size in rice.

OsCLV2a regulates grain size and confers *indica*−*japonica* differentiation

To explore the genetic function of *OsCLV2a*, the highest homology with CLV2 in Arabidopsis by phylogenetic tree analysis and domain analysis of *OsCLV2s* (Fig. S5), we performed the haplotype analysis and the result showed that the accessions could be classified into 8 haplotypes based on the polymorphisms, with 1791

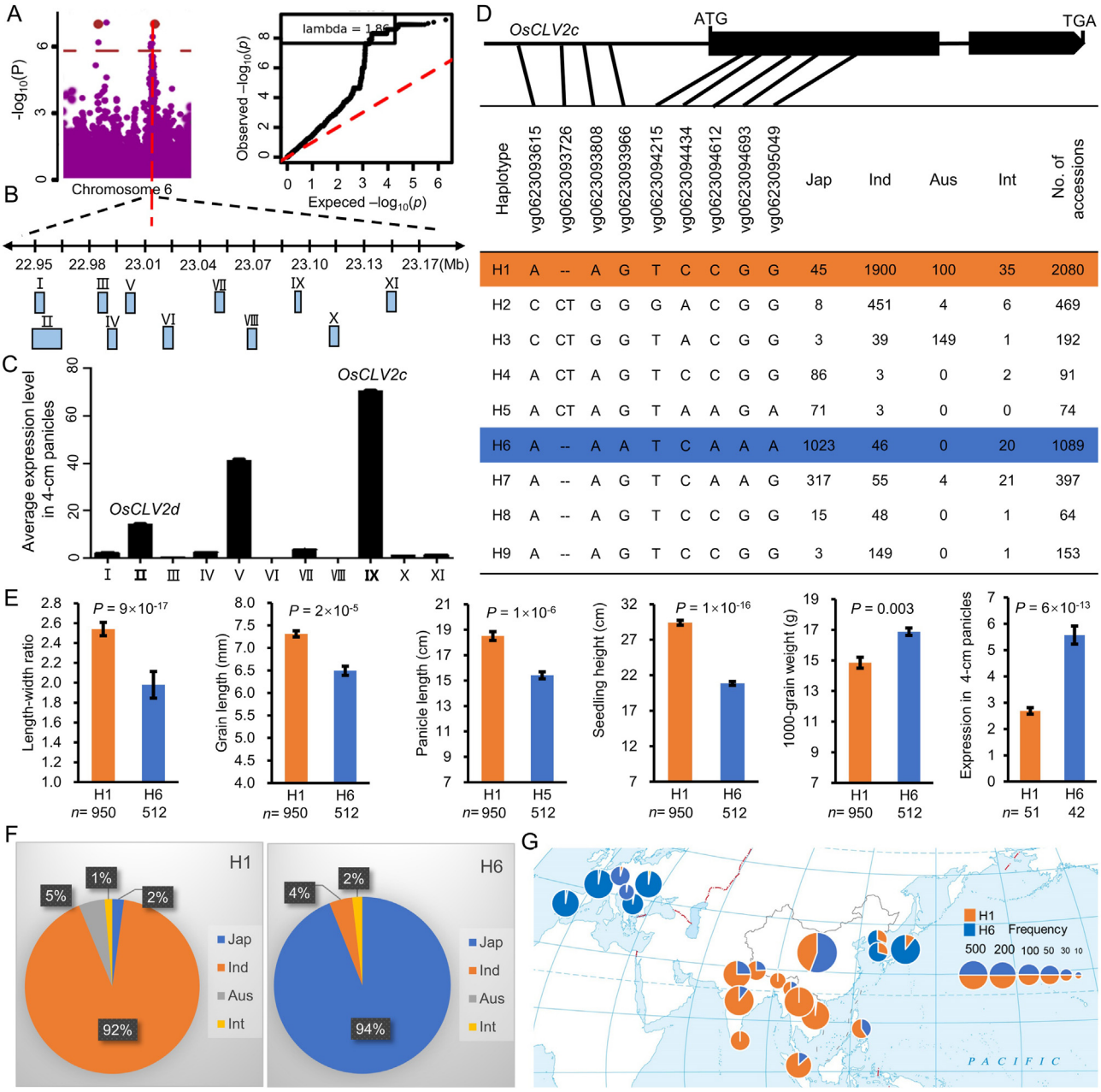

Fig. 1. Identification and haplotype analysis of *OsCLV2c* for grain shape. **A**: Manhattan and quantile−quantile plots for GWAS of grain shape/grain length−width ratio on chromosome 6. **B**: The underlying candidate genes within the 200-Kb region around the peak. **C**: Average expression levels of all possible candidate genes in 4-cm panicles of the rice mini-core collection of 533 accessions. **D**: The representative variations in the promoter and coding region of *OsCLV2c* in the rice 4726 accessions were classified into nine haplotypes. **E**: The difference of grain length−width ratio, grain length, panicle length, seeding height, and 1000-grain weight in 4726 accessions, as well as expression levels in 4-cm panicles in 533 accessions between the two major haplotypes of *OsCLV2c*. **F**: The analysis of *indica*−*japonica* differentiation of the major haplotypes H1 and H6. **G**: The analysis of geographical distribution of H1 and H6 using rice 4726 accessions (Zhao et al., 2021). The figure is based on the standard map with the ID GS(2016)2962 that was taken from the website of the National Platform for Common Geospatial Information Services. Jap, Ind, Aus, and Int represent *japonica*, *indica*, *aus*, and *intermediate* accessions, respectively. *n* is the number of accessions. All data are shown as mean value ± SEM. All the *P* values were produced by two-tailed *t*-tests. GWAS, genome-wide association studies; SEM, standard error of mean.

accessions carrying H1 and 827 accessions carrying H5 (Fig. 3A; Table S5). There were significant differences in grain size between the two major haplotypes (H1 and H5) (Fig. 3B), as well as its predominant expression pattern in panicles (Fig. S6), hitting that *OsCLV2a* may contribute to grain shapes in rice. The haplotype network analysis of *OsCLV2a* suggested it may contribute to *indica*−*japonica* differentiation (Fig. S7). Furthermore, 1639 out of 1791 accessions (92%) of H1 were *indica* rice, while 790 out of 827 accessions (95%) of H5 could be distinctly classified to *japonica* rice (Fig. 3C), hitting that *OsCLV2a* differentiates between *indica* and *japonica*. Then, the major haplotypes of *OsCLV2a* showed a distant geographical distribution: H1 is mainly found in South American and Southeast Asian countries, while H5 is mostly found in Southwestern Europe and East Asia (Fig. 3D). In brief, *OsCLV2a* may regulate grain size and confer greatly on the *indica*−*japonica* differentiation and geographical distribution in rice.

To further characterize the genetic effect of the above *CLV2* homologous genes on grain size in rice, we generated *OsCLV2a/c/d* triple mutants and *osclv2a/f* double mutants in ZH11. Phenotypic analyses showed that independent mutant lines of *osclv2a/c/d* and

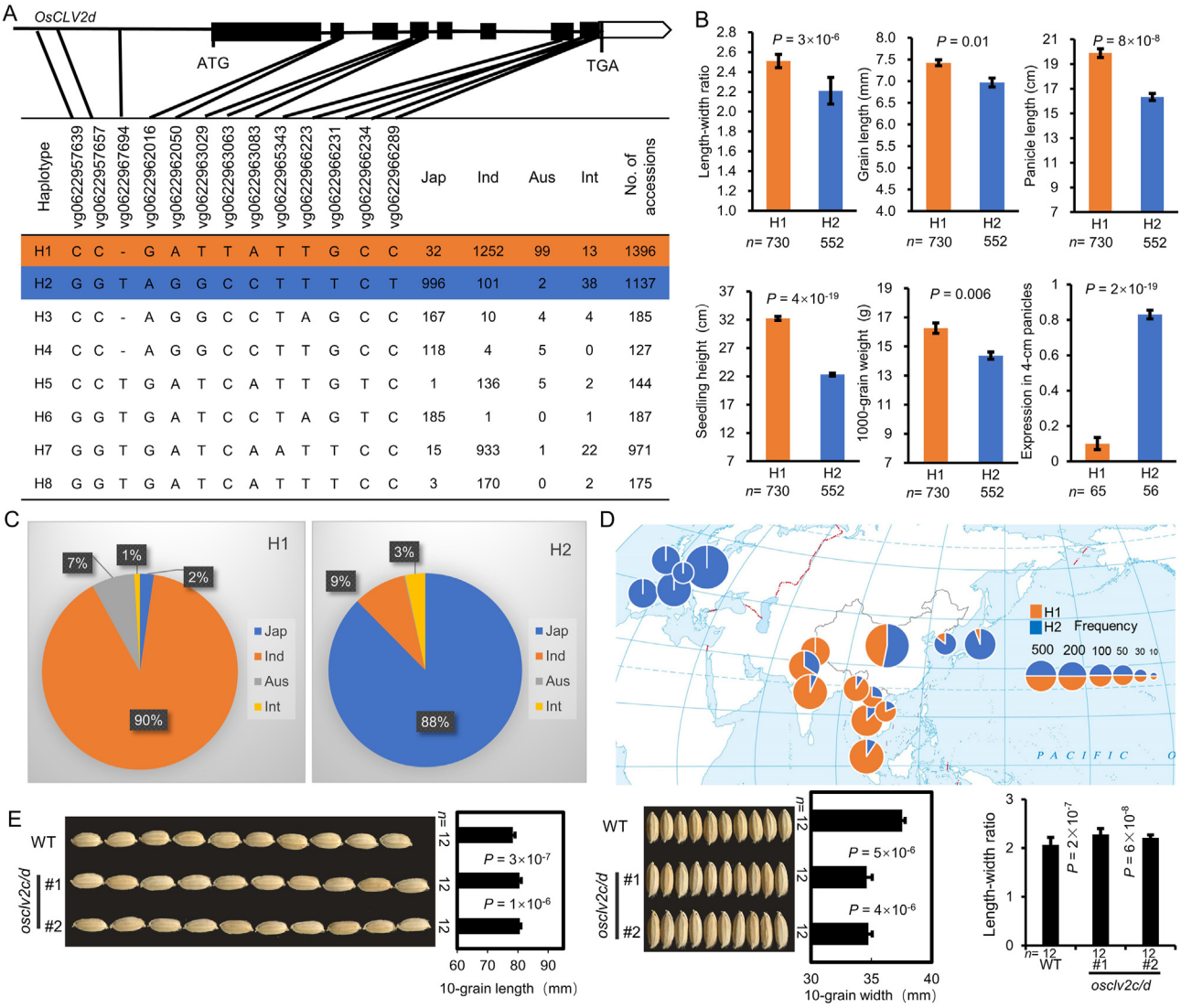

Haplotype	vg0622957639	vg0622957657	vg0622967694	vg0622962016	vg0622962050	vg0622963029	vg0622963063	vg0622963083	vg0622965343	vg0622966223	vg0622966231	vg0622966234	vg0622966289	Jap	Ind	Aus	Int	No. of accessions
H1	C	C	-	G	A	T	T	A	T	T	G	C	C	32	1252	99	13	1396
H2	G	G	T	A	G	G	C	C	T	T	T	C	T	996	101	2	38	1137
H3	C	C	-	A	G	G	C	C	T	A	G	C	C	167	10	4	4	185
H4	C	C	-	A	G	G	C	C	T	T	G	C	C	118	4	5	0	127
H5	C	C	T	G	A	T	C	A	T	T	G	T	C	1	136	5	2	144
H6	G	G	T	G	A	T	C	C	T	A	G	T	C	185	1	0	1	187
H7	G	G	T	G	A	T	C	A	A	T	T	C	C	15	933	1	22	971
H8	G	G	T	G	A	T	C	A	T	T	T	C	C	3	170	0	2	175

Fig. 2. Haplotype analysis of *OsCLV2d* and function confirmation of *OsCLV2c* and *OsCLV2d*. **A**: The representative variations in the promoter and coding region of *OsCLV2d* in the rice 4726 accessions were classified into 8 haplotypes. **B**: The difference of grain length−width ratio, grain length, panicle length, seeding height, and 1000-grain weight in 4726 accessions, as well as expression levels in 4-cm panicles in 533 accessions between the two major haplotypes of *OsCLV2d*. **C**: The analysis of *indica*−*japonica* differentiation of the major haplotypes H1 and H2. **D**: The analysis of geographical distribution of H1 and H2 using the rice 4726 accessions. The figure is based on the standard map with the ID GS(2016)2962 that was taken from the website of the National Platform for Common Geospatial Information Services. **E**: Grain shape of the *OsCLV2c/d* double mutants in T_2 progenies. Jap, Ind, Aus, and Int represent *japonica*, *indica*, *aus*, and *intermediate* accessions, respectively. *n* is the number of accessions or the number of individuals of each transgenic line. All data are shown as mean value ± SEM. All the *P* values were produced by two-tailed *t*-tests. SEM, Standard error of mean.

osclv2a/f also exhibited longer and narrower grains than those of the wild type (Figs. 3E and S8). Taken together, these results confirm that these homologous genes of *OsCLV2s* negatively regulate grain shape in rice.

OsCRN1 differentiating *indica*−*japonica* accessions controls grain size

Another significant QTL on chromosome 1 was also discovered for grain length−width ratio, and 15 possible candidate genes at the GWAS peak locus were identified (Fig. 4A; Table S6). Among them, the gene *LOC_Os01g70260* (IV, *OsCRN1*) predominantly and uniquely expressed in young panicles was identified as the candidate gene (Figs. 4B and S9). The haplotype analysis using 4726 accessions identified 7 haplotypes (H1−H7) determined by 10 major representative variations of *OsCRN1* (Fig. 4C; Table S7). Moreover, there existed an obvious difference in grain length−width ratio, grain length, grain width, and expression pattern in 1-mm panicles between the two haplotypes of *OsCRN1* (Fig. 4D), suggesting *OsCRN1* presumably regulates grain size development in rice. The haplotype network analysis of *OsCRN1* in the 4726 accessions suggested *OsCRN1* may contribute to the *indica*−*japonica* differentiation (Fig. S10). Subsequently, the two major haplotypes of *OsCRN1*, H1 ($n = 1209$) and H3 ($n = 2522$) had distinct advantages in the *japonica* (96%) and *indica* (91%) subspecies, respectively (Fig. 4E), showing that *OsCRN1* also shows the *indica*−*japonica* differentiation. H1 is primarily found in European and East Asian countries, while H3 is mostly located in Southeast Asian countries (Fig. 4F), which also shows significant geographical distribution differentiation of the main haplotypes of *OsCRN1* in rice.

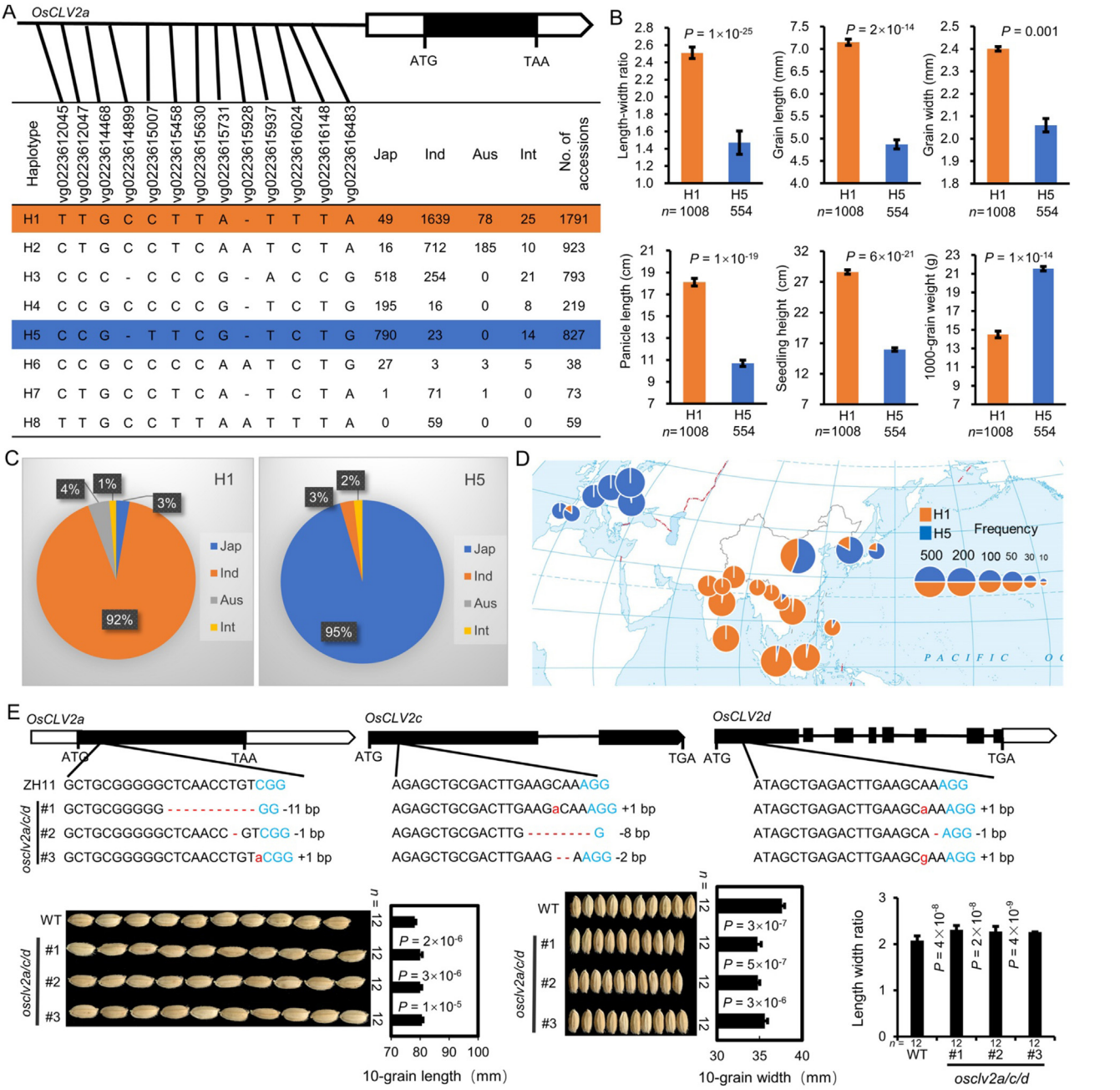

Fig. 3. Haplotype and geographical distribution analysis of *OsCLV2a* and function confirmation of *OsCLV2a/c/d*. **A**: The representative variations in the promoter of *OsCLV2a* in the rice 4726 accessions. **B**: The difference of grain length–width ratio, grain length, grain width, panicle length, seeding height, and 1000-grain weight between the two major haplotypes of *OsCLV2a* in 4726 accessions. **C**: The analysis of *indica–japonica* differentiation of the major haplotypes H1 and H5 of *OsCLV2a*. **D**: The analysis of geographical distribution of H1 and H5 of *OsCLV2a* in the rice 4726 accessions. The figure is based on the standard map with the ID GS(2016)2962 that was taken from the website of the National Platform for Common Geospatial Information Services. **E**: The genotypes and grain-shape phenotypes of the *osclv2a/c/d* triple mutants compared with ZH11 in T_2. #1, #2, and #3 represented the independent CRISPR/Cas9 lines. Jap, Ind, Aus, and Int represent *japonica*, *indica*, *aus*, and *intermediate* accessions, respectively. *n* is the number of accessions or the number of individuals of each transgenic line. All data are shown as mean value ± SEM. All the *P* values were produced by two-tailed *t*-tests. GWAS, genome-wide association studies; SEM, standard error of mean.

OsCLV2a interacts with OsCRN1 biochemically and genetically

To confirm whether OsCLV2s work together with OsCRN1, we designed a serials of genetic and biochemical experiments. As the transcripts of *OsCLV2c* and *OsCLV2d* containing kinase domains are too long to be successfully cloned using various protocols (Fig. S5B), we used *OsCLV2a* for further analysis. OsCLV2a contains seven leucine-rich repeat (LRR)-repeat domains and a transmembrane domain anchored in the extracellular membrane through the C terminal, while OsCRN1, homologous to *CRN* in Arabidopsis, consists of a kinase domain and a transmembrane domain anchored in the intracellular membrane through the N terminal (Figs. S5 and S11), suggesting that they may form a complex via their transmembrane domains in signal transduction pathways. To verify their physical interaction, we conducted split luciferase complementation and pull down assays, and the results suggested that OsCLV2a interacted with OsCRN1 in vivo and in vitro via their transmembrane domains (Figs. 5A, 5B, S12). To confirm the genetic function of *OsCLV2a* and *OsCRN1* in regulating the grain size in vivo, we obtained the single

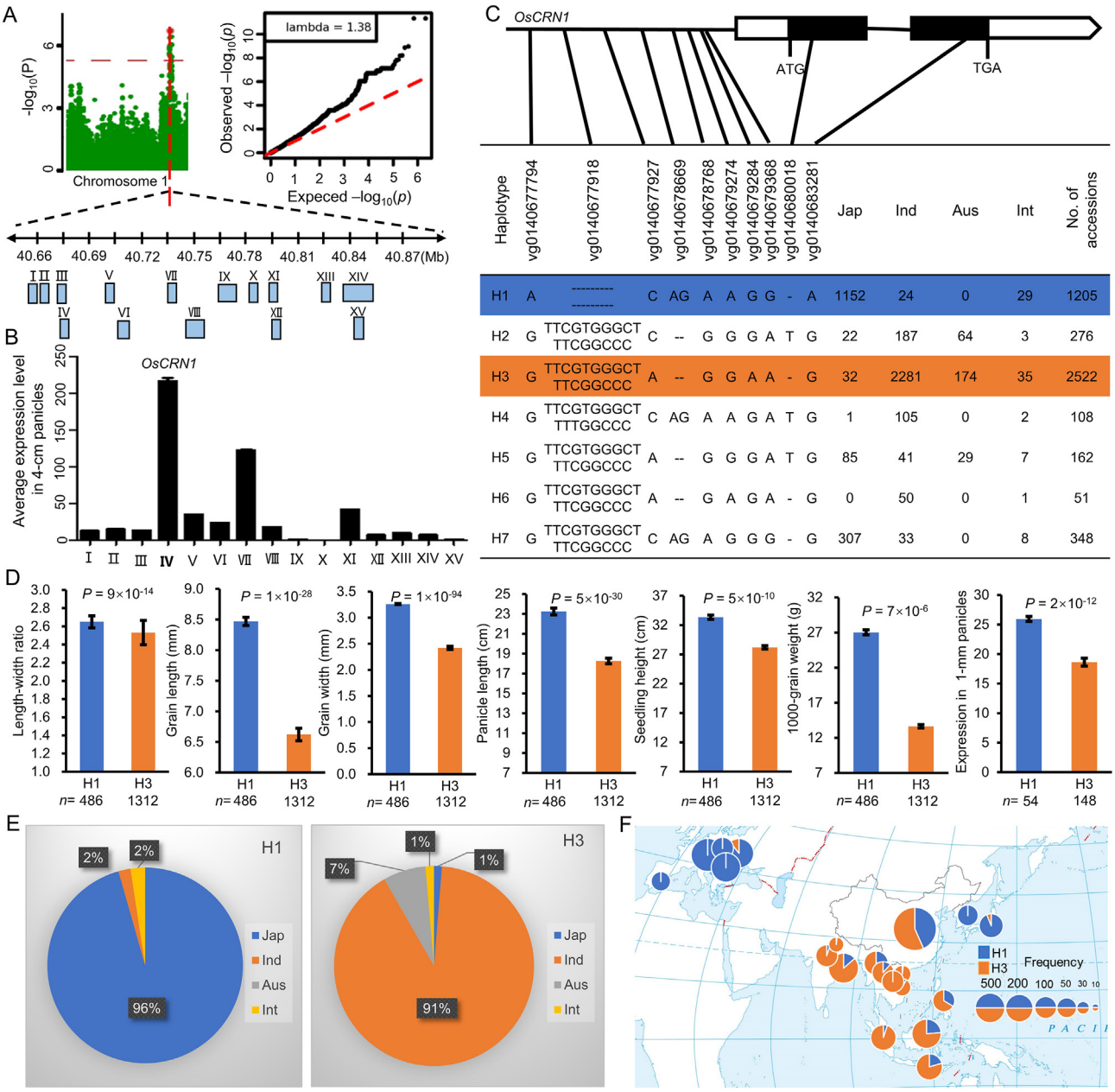

Fig. 4. Identification of *OsCRN1* by GWAS and its haplotype and geographical distribution analysis. **A**: Manhattan and quantile−quantile plots for GWAS of grain shape/grain length−width ratio on chromosome 1 and the location of the predicted ORFs around the peak. **B**: Average expression levels of all candidate genes in 4-cm panicles of the rice mini-core collection. **C**: The representative variations in the promoter and coding region of *OsCRN1* in the rice 4726 accessions were classified into eight haplotypes. **D**: The difference of grain length-width ratio, grain length, grain width, panicle length, seeding height, and 1000-grain weight between the two major haplotypes of *OsCRN1* in 4726 accessions. **E**: The analysis of *indica*−*japonica* differentiation of the major haplotypes H1 and H3 of *OsCRN1*. **F**: The analysis of geographical distribution of H1 and H3 of *OsCRN1* in 4726 accessions. The figure is based on the standard map with the ID GS(2016)2962 that was taken from the website of the National Platform for Common Geospatial Information Services. Jap, Ind, Aus, and Int represent *japonica*, *indica*, *aus*, and *intermediate* accessions, respectively. *n* is the number of accessions. All data are shown as mean value ± SEM. All the *P* values were produced by two-tailed *t*-tests. GWAS, genome-wide association studies; SEM, standard error of mean.

mutants of *OsCLV2a* and *OsCRN1* and their double mutants (Fig. 5C). All these mutants showed similar trends in grain shape: increased grain length−width ratios coupled with increased grain length and decreased grain width (Figs. 5D and S13), indicating that *OsCRN1* and *OsCLV2s* possess similar functions in grain shape regulation in rice. Taken together, these data confirmed that *OsCLV2a* and *OsCRN1* work together for grain shape control in rice.

OsCLV2a, *OsCLV2c*, *OsCLV2d*, and *OsCRN1* experienced artificial selection

To further seek the relationships among *OsCLV2a*, *OsCLV2c*, *OsCLV2d*, and *OsCRN1*, we conducted the genetic contribution analysis of their haplotypes to grain yield traits and their domestication analysis. Firstly, the in-depth haplotype analysis combining

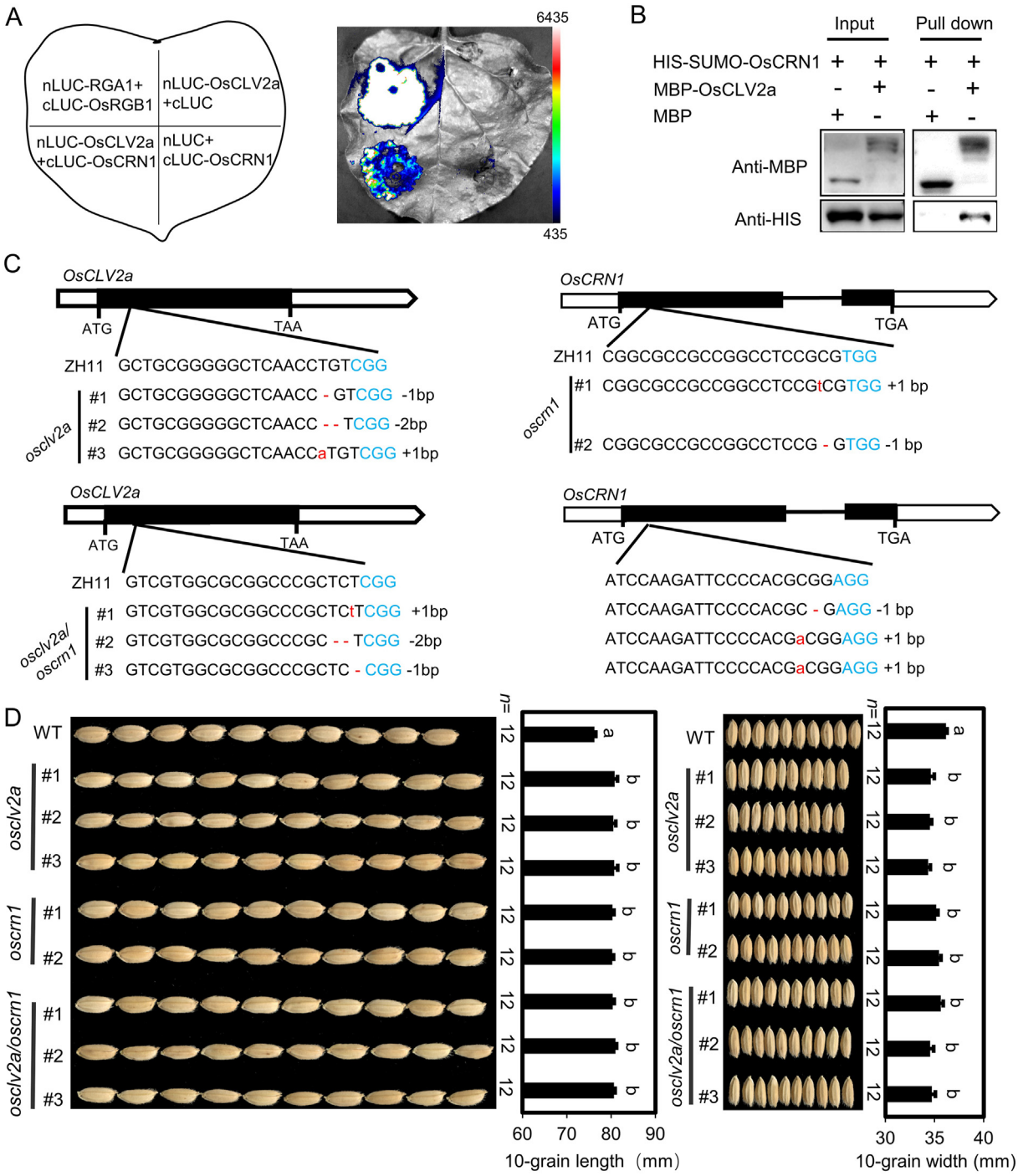

Fig. 5. OsCLV2a interacted with OsCRN1 biochemically and genetically. **A**: Split-LUC assays verified the interaction of OsCLV2a and OsCRN1. nLUC-RGA1 and nLUC-OsRGB1 were presented as a positive control. **B**: Pull-down assays checked the interaction of OsCLV2a and OsCRN1. MBP were presented as a negative control. **C**: The sgRNA target sites and genotypes of the single mutants of *osclv2a*, *oscrn1*, and their double mutants of *osclv2a*/*oscrn1* by CRISPR/Cas9 in ZH11. PAM sequences are marked in blue. **D**: Grain shape of *OsCLV2a*, *OsCRN1*, and *OsCLV2a*/*OsCRN1* mutants compared with the wild type ZH11. *n* is the number of individuals of each transgenic line. All data are shown as mean value ± SEM. All the *P* values were produced by two-tailed *t*-tests. SEM, standard error of mean.

the 3 genes (*OsCLV2a*, *OsCLV2c*, and *OsCRN1*) together identified 8 haplotypes based on their representative variations in 4726 accessions (Fig. 6A). Furthermore, there is a significant difference between the two major haplotypes H3 and H4 in grain shape, panicle length, 1000-grain weight, and grain yield (Fig. 6B), indicating that the two major haplotypes have important functions on grain yield traits in rice. To evaluate the genetic contribution of these haplotypes to the major yield traits of rice, we performed the ANOVA analysis using the representative variant genotypes and haplotypes of the three genes and grain yield traits in 533 accessions (Fig. 6C). The results showed that they explained 4.36%–11.21% of grain shape variation, 2.35%–10.23% of grain length variation, 1.13%–12.01% of grain width variation, 1.52%–12.36% of length–width ratio variation, 1.42%–9.36% of seedling height variation, 4.43%–10.68% of 1000-grain weight variation, 2.52%–8.23% of grain number variation, 1.67%–9.68% of panicle length variation, 10.01%–18.65% of grain yield

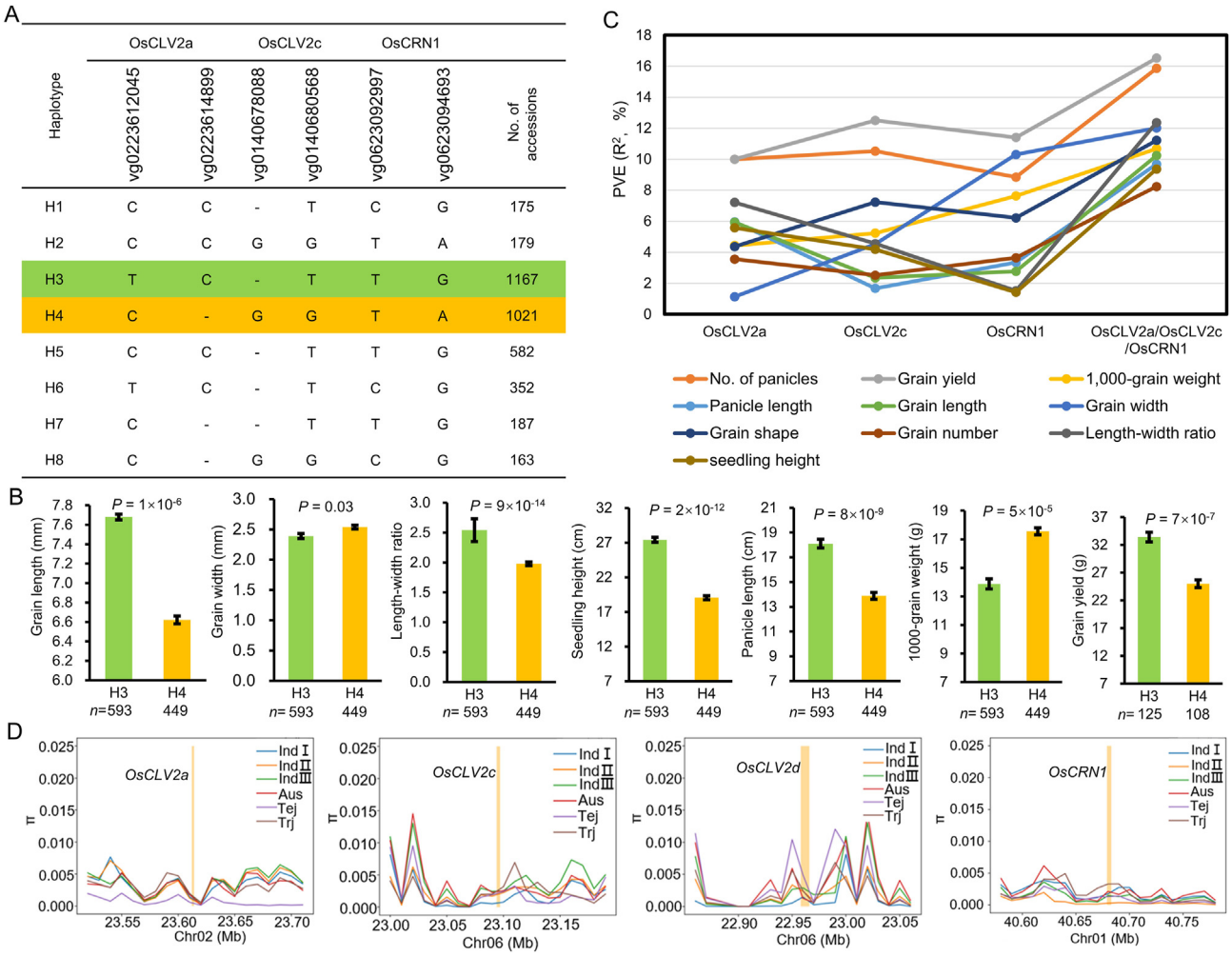

Fig. 6. The genetic contributions and selection signatures of *OsCLV2a*, *OsCLV2c*, *OsCLV2d*, and *OsCRN1*. **A**: Haplotype analysis of the three genes (*OsCLV2a*, *OsCLV2c*, and *OsCRN1*) together using the rice 4726 accessions. **B**: Phenotype difference between two major haplotypes H3 and H4 in 4726 accessions. **C**: Genetic contributions of these three genes by ANOVA analysis using their representative variants and grain yield traits in 4726 accessions. **D**: The selection signatures in 200-kb region sequences of the *OsCLV2a*, *OsCLV2c*, *OsCLV2d,* and *OsCRN1* from a panel of 3216 accessions. Ind I, Ind II, Ind III, Aus, Tej, and Trj represent *Indica* I, *Indica* II, *Indica* III, *Aus*, *Temperate japonica*, and *Tropical japonica* accessions, respectively. *n* is the number of accessions. All data are shown as mean value ± SEM. All the *P* values were produced by two-tailed *t*-tests. SEM, standard error of mean. PVE, phenotype variance explanation.

variation in the rice mini-core collection (Fig. 6C). Furthermore, the genetic contributions of the haplotypes combining the three genes together to yield traits were much higher than those of single genes (Fig. 6C). These results suggested that the haplotypes of the three genes had synergistic and great effects on the variation of yield traits in rice. Secondly, to explore whether these four genes had undergone artificial selection during rice domestication, we analyzed the selection signatures in the 200-kb region sequences of the four genes from a panel of 3216 accessions. The selection signatures revealed their low nucleotide diversity for each of the four genes (Fig. 6D), which indicated that they experienced different degrees of artificial selection during rice domestication. Taken together, *OsCLV2a*, *OsCLV2c*, *OsCLV2d*, and *OsCRN1* contribute greatly to *indica*–*japonica* differentiation and geographical distribution in rice, and they experienced artificial selection.

Discussion

Comprehending grain size/shape control in rice is key to breeding high-yield varieties by optimizing growth and development processes and remains elusive. Although some QTL or QTGs regulating rice grain shape have been identified (Fan and Li, 2019; Li et al., 2019; Zhang et al., 2021), it remains to be checked whether the *CLV* homologous genes regulate grain shape/size in rice. In this study, we identify four genes: *OsCLV2a*, *OsCLV2c*, *OsCLV2d*, and *OsCRN1* underlying natural variation in rice, and these genes negatively regulate grain shape/grain lengthwidth ratio (Figs. 1–4). This observed phenotype is reminiscent of those seen in the *CLV* mutants, such as *THICK TASSEL DWARF1* (*TD1*, *CLV1* ortholog) and *FASCIATED EAR2* (*FEA2*, *CLV2* ortholog) for yield traits, especially tassel spikelet density and kernel row number in maize (Fletcher, 2018). The *fasciated and branched* (*fab*) mutant develops branched inflorescences with fasciated flowers as a consequence of enlarged meristems and larger fruits (Xu et al., 2015). Notably, we find that *OsCLV2c* and its homologous *OsCLV2d* are co-located in a GWAS peak as a cluster QTL (Figs. 1 and 2). Convincingly, these genes all function as negative regulators of grain length-width ratio in rice. All these results indicate that the *CLV*-like genes regulating yield traits are evolutionarily conserved in crops, which implies that we could design elaborately to foster high-yield varieties of rice by utilizing the mechanisms on the CLV–WUS pathway in other species.

CLV2 could indeed interact with CRN biochemically to form a tetramer receptor complex, and they require each other for exporting from the endoplasmic reticulum and locating to the plasma membrane (PM) in Arabidopsis (Bleckmann et al., 2010; Meng and Feldman, 2010; Zhu et al., 2010). In addition, the defective carpel and siliques phenotypes of *clv2* were similar to that of *crn* (Müller et al., 2008; Bleckmann et al., 2010), and the flower primordia outgrowth phenotypes of *clv2/crn* double mutants were similar to those of *clv2* or *crn* single mutants (Jones et al., 2021), indicating that *CLV2* and *CRN* act in the same pathway for controlling the reproductive development in Arabidopsis. Another research reported that *ZmCRN* and *FEA2* function in a common pathway in maize (Je et al., 2018). Similarly, in this study, we found that *OsCLV2s* and *OsCRN1*, the highest homology with *CLV2* and *CRN* in Arabidopsis, respectively (Figs. S5 and S11), are membrane proteins co-localized in the membrane and may form a complex via their transmembrane domains to play a similar role with those in Arabidopsis. Subsequently, the OsCLV2a was selected to represent OsCLV2s to verify its connection with OsCRN1 biochemically and genetically in vivo and in vitro (Fig. 5). Thus, it can be deduced that there exist the conserved elements and mechanisms in the CLV−WUS pathway for grain shape in rice. The protein kinase family possess the conserved features of the catalytic domains (Hanks et al., 1988). Here, OsCRN1, without the Asp(D)-Phe (F) -Gly (G) in subdomain VII(DFG) motif that determines the kinase activity (Fig. S14), is likely a pseudo-kinase, which is similar to CRN in Arabidopsis. It is likely that CRN could transmit the CLE peptide signal, neither functioning as a scaffolding protein nor solely localizing CLV2 to the PM (Somssich et al., 2016b). CLV2/CRN may interact with CLV1, CIKs, and RPK2 to achieve the signal transmission (Somssich et al., 2015; Shinohara and Matsubayashi, 2015; Hu et al., 2018). Therefore, it could be speculated that an unknown partner or kinase co-localizing with OsCLV2s/OsCRN1 in membrane acts as a linker or co-receptor of them. Moreover, OsCLV2c/d/e/f possess the kinase catalytic domains in despite of several variations (Figs. S5 and S15), implying that they may function as kinases. It is also essential for OsCLV2s/OsCRN1 to pass the signal to unknown downstream effectors.

Based on our findings and speculations, we proposed a model of two types of receptor-like kinases to understand the molecular mechanisms of the CLV−WUS pathway in rice (Fig. 7): the extracellular OsCLV2a/b and intracellular OsCRN1 without kinase activity, probably form an integral receptor or complex with an unknown kinase to perceive and transmit unknown signals to effectors to produce the short and wide grains; OsCLV2c/d/e/f, consisting of LRR and kinase domains, interacts with OsCRN1 to achieve signal transduction to effectors likely without an unknown kinase partner. In the mutants, these interactions are broken to produce long and thin grains (Fig. 7). This study provides a framework to understand the CLV−WUS pathway in rice for altering stem cell activity to control grain size. The real relationship between OsCRN1 and other OsCLV2s for their genetic and biochemical functions needs further investigations in the near future, which can fill the molecular mechanism gaps of the CLV−WUS feedback loop in rice.

In maize, the *CLV*-like receptors (*TD1* and *FEA2*) regulating yield traits are likely to have been targets of selection during maize domestication (Bommert et al., 2005, 2013; Fletcher, 2018). In addition, the variation of the *fascinated* (*fas*, the *CLV3* ortholog) in tomato has been selected during breeding and domestication for cultivars with increased fruit size (Fleming 2015; Xu et al., 2015). Here, based on the in-depth haplotype analysis of *OsCLV2a*, *OsCLV2c*, *OsCLV2d*, and *OsCRN1* using the rice 4726 accessions and the geographical distribution of the primary haplotypes, we learn that the major haplotype H1 of *OsCLV2a*, *OsCLV2c*, and *OsCLV2d* as well as H3 of *OsCRN1* with absolute advantages in *indica* accessions are mainly found in Southeast Asian countries; while the major haplotypes, H5 of *OsCLV2a*, H6 of *OsCLV2c*, H2 of *OsCLV2d*, and H1 of *OsCRN1* with distinct advantages in *japonica*, are predominantly found in Europe and East Asia (Figs. 1G, 2D, 3D, 4F). These results indicate that the haplotype H1 of *OsCLV2a*, *OsCLV2c*, and *OsCLV2d* may work together with the haplotype H3 of *OsCRN1* in *indica* subspecies, while the haplotypes H5 of *OsCLV2a*, H6 of *OsCLV2c*, H2 of *OsCLV2d*, and the haplotype H1 of *OsCRN1* may coexist in *japonica* accessions. In addition, the genetic contributions of the whole haplotypes combining *OsCLV2a*, *OsCLV2c*, and *OsCRN1* together to many yield traits in a mini-core collection are much higher than that of every single gene (Fig. 6C). Furthermore, *OsCLV2a*, *OsCLV2c*, *OsCLV2d*, and *OsCRN1* all experienced the different degrees of artificial selection during rice domestication (Fig. 6D). Taken together, these findings imply that *OsCLV2a*, *OsCLV2c*, *OsCLV2d*, and *OsCRN1* contribute to the *indica*−*japonica* differentiation and were selected together during rice domestication, as well as may work together in seed development to play an important role in grain shape control in rice. It can be speculated that the *CLV*-like receptors are the targets of artificial selection during domestication, which is conserved in crops, such as maize, tomato and rice.

CRISPR/Cas9 genome engineering strategy was used to generate diverse *cis*-regulatory alleles in the promoter of *fas/SlCLV3*,

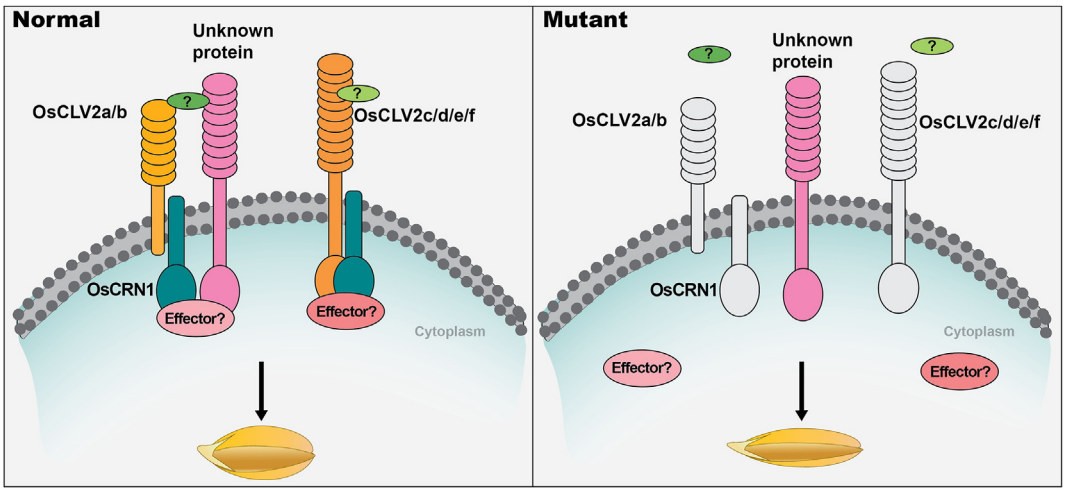

Fig. 7. A proposed model of OsCLV2s and OsCRN1 in regulating grain size in rice.

which provides the beneficial quantitative variation for breeding and allows the fixation of new alleles and fines manipulation of yield components (Rodríguez-Leal et al., 2017). In addition, de novo domestication of wild tomatoes using targeted reverse genetic engineering of coding sequences, *cis*-regulatory regions, or upstream open reading frames of genes including *fas*/*SlCLV3* and *locule number* (*lc*, the *WUS* homologs), associated with morphology, flower and fruit production, and ascorbic acid synthesis, could rapidly create new crops and avoid the loss of genetic diversity in crop improvement by inbreeding (Li et al., 2018; Zsögön et al., 2018). In this study, many natural variations in promoter regions of *OsCLV2a*, *OsCLV2c*, *OsCLV2d*, and *OsCRN1* contribute to their expression differences and grain shape variation in rice. So it can be speculated that the *OsCLV2s* and *OsCRN1* may possess the potential for grain-size improvement via targeted genetic modifications, which provides a unique insight into the optimization of breeding high-yield varieties in rice.

It is reported that the important components of the CLV−WUS pathway in rice play a significant role in stem cell maintenance, specifically in floral or vegetative meristems (Hong and Fletcher, 2023). But in this study, we report a group of receptor-like kinases that may function as co-receptors to regulate grain shape in rice, thereby revealing a previously unrecognized role of the *CLV* class genes in regulating seed development and providing important genetic resources to breed high-yield varieties in rice and other crops. This work provides a new insight into the molecular mechanism of the CLV−WUS pathway in rice and encourages more researchers to invest in the further exploitation of this pathway.

Materials and methods

Genome-wide association study

Genome-wide association study (GWAS) analysis using grain length−width ratio phenotype of the rice mini-core collection, containing 533 accessions worldwide were performed by the factored spectrally transformed linear mixed model (FaST-LMM) (Lippert et al., 2011), in which all genotypes of the 533 accessions were downloaded from the RiceVarMap v2.0 database (http://ricevarmap.ncpgr.cn) (Zhao et al., 2015, 2021). There are 4,131,700 single nucleotide polymorphism (SNPs) for GWAS analysis, after filtering out some SNPs with minor allele frequency (MAF) $< 5\%$. The Manhattan plots were mapped by the *qqman* package. The Bonferroni correction was used to evaluate the threshold for genome-wide significance ($P = 0.05/n$ after correction, n is the effective number of independent single nucleotide polymorphisms (SNPs) in the whole genome). The n was estimated by pruning the SNP dataset using PLINK (version 1.9) (Purcell et al., 2007). The genome-wide significance level for grain size was determined as 1.37×10^{-6}.

Natural variation and haplotype analysis

All the natural variations in the 2-kb promoter regions, the coding, and the 0.5-kb downstream regions of *OsCLV2a*, *OsCLV2c*, *OsCLV2d*, and *OsCRN1* from 533 rice accessions downloaded from the RiceVarMap v2.0 database (http://ricevarmap.ncpgr.cn) (Zhao et al., 2015; 2021) and RFGB v2.0 database (https://www.rmbreeding.cn/Index/) (Wang et al., 2020). Haplotype analyses were performed using all the representative variations. All the natural variations and representative variations of rice accessions are listed in Tables S3, S4, S5 and S7.

Haplotype network analysis

All the SNP genetic variations (the number of SNPs < 100) of *OsCLV2a*, *OsCLV2c*, *OsCLV2d*, and *OsCRN1* obtained in RiceVarMap v2.0 (http://ricevarmap.ncpgr.cn/) (Zhao et al., 2021) and RFGB v2.0 (https://www.rmbreeding.cn/Index/) (Wang et al., 2020) were entered into the haplotype network analysis in the tools to generate haplotype plots. A total of four groups, *Indica*, *Japonica*, *Aus*, and intermediate, were used. *Indica* group includes *Indica* I, *Indica* II, *Indica* III, and *Indica* intermediate; *Japonica* group includes *temperate Japonica*, *tropical Japonica*, and *Japonic* intermediate; intermediate group includes Aromatic and other accessions.

Field growth conditions and grain size measurement

All the materials used in this study were grown in the experimental field of Huazhong Agricultural University in Lingshui (Hainan province, China) from December to May or in Wuhan (Hubei province, China) from May to October. The plants subjected to normal field management, such as fertilizer application, irrigation and pest control. Filled grains from each plant were randomly chosen, and the data of 10-grain length and 10-grain width of all the materials were obtained using a vernier caliper. Then the grain length-width ratio was calculated as an indicator of grain shape in rice.

Vector construction and generation of transgenic plants

All the mutant materials were generated by the CRISPR/Cas9 gene editing technique (Gao and Zhao, 2014). For the construction of the CRISPR vectors of *OsCLV2a*/*c*/*d*, *OsCLV2a*/*f*, *OsCLV2a*, *OsCRN1*, and *OsCLV2a*/*OsCRN1*, the specific 20nt sgRNAs, excluding the possibility of off-target were designed and cloned into the CRSPR/Cas9 binary expression vector, respectively. All the CRISPR vectors were generated through homologous recombination by one-step enzymatic assembly of DNA molecules with the In-Fusion cloning kit (Vazyme Biotech) and confirmed by the sequencing analysis. The vectors were transformed into ZH11 callus by *Agrobacterium tumefaciens*-mediated transformation. The positive plants were selected by hygromycin resistance. All the sgRNA targets were listed in Table S8.

Genotypes of the CRISPR transgenic lines

DNA polyacrylamide gel electrophoresis and gene sequencing were used to identify the genotypes of all the CRISPR/Cas9 mutant materials. In details, polymerase chain reaction (RCR) products with about 100-bp length were obtained using the specific primers and separated by 6% PAGE gel. And 3−5 independent mutant lines were chosen and sequenced to ensure frameshift mutants. All the primers for genotyping were listed in Table S8.

Phylogenetic analysis and domain prediction

OsCLV2s, *OsCRN1*, and their homologs and orthologues in rice or other plant species using BLAST servers such as databases of NCBI (http://blast.ncbi.nlm.nih.gov) and MSU (http://rice.plantbiology.msu.edu/index.shtml). Phylogenetic tree was constructed with the aligned protein sequences using MEGA 7.0 (http://www.megasoftware.net/index.html) and using the neighbor-joining (NJ) method with the following parameters: Poisson correction, pairwise deletion, and bootstrap resampling 1000 times. All candidate genes

were examined by domain prediction servers SMART (https://smart.embl.de/).

The phenotype variance explanation (PVE)

The phenotype data of grain shape, grain length, grain width, 1000-grain weight, panicle length, grain number, and grain yield per plant of the 533 accessions were obtained. The grain yield trait values of the mini-core collection were listed in Table S1. The PVE was determined by the one-way or multiple ANOVA using the haplotypes of each gene (*OsCLV2a*, *OsCLV2c*, and *OsCRN1*) and these genes together as the predictor variables and the phenotypes of grain yield traits in 533 accessions, which were used to assess the genetic contribution.

Luciferase complementation assay

Full-length coding sequence (CDS) fragments of OsCLV2a was fused in the N terminal of nLUC and OsCRN1 was cloned in the N terminal of cLUC vectors, respectively (Chen et al., 2008). The vectors were transformed into *Agrobacterium* strain EHA105, respectively. The bacteria with the same concentration were mixed as required and coinfiltrated into 3-week-old tobacco (*Nicotiana benthamiana*) leaves. After expressed two days, the leaves were injected with 1 mM luciferin (Promega, E1605) for 5 min, and the luciferase signals were observed using cooled charge coupled device (CCD)-imaging apparatus (Tanon 5200). Three independent experiments were repeated. Primers used in this assay were listed in Table S8.

Pull-down assay

The full-length OsCLV2a and OsCRN1 were inserted into the *pMar-c2X* vector and *pET28a-SUMO* vector, respectively. The recombinant vectors maltose binding protein (MBP), MBP-OsCLV2a, and His-SUMO-OsCRN1 were transformed into *E. coli* BL21 (DE3) cells using chemical transformation mediated by calcium chloride, and the plates were cultivated at 37°C for 12 h−16 h. The bacterial colony were collected into 5 mL LB medium and shaken at 37°C for 5 h−8 h. Subsequently, the solutions were transformed into 200 mL LB medium and shaken at 37°C for 2 h−3 h, the OD600 of the bacterial fluid was approximately 0.6−0.8. The recombinant proteins were induced for expression after culturing for 16 h−18 h in LB medium by the addition of 1.0 mM isopropylthio-β-galactoside (IPTG) with 160-rpm shaking at 16°C. Then, bacterial cells were collected by centrifugation at 4000 rpm for 10 min at 4°C and resuspended by adding 10 mL lysis buffer. After that, the bacteria were broken using an ultrasonic crusher in low-temperature environments, and the protein lysis was obtained by centrifugation at 12,000 rpm for 30 min at 4°C. Furthermore, the concentration and purity of proteins were determined by a 12% SDS-PAGE gel.

The lysis was mixed as required and incubated for 6 h at 4°C. Then, it is needed to stay for 3 h at 4°C after adding MBP beads. The beads were washed five times with washing buffer and then boiled with SDS loading buffer for 5 min. The samples were separated by SDS-PAGE and subjected to immunoblotting using an anti-MBP antibody (Abclone; AE016, 1:5000 dilution) and an anti-His antibody (Biodragon; B1004, 1:10,000 dilution). Primers used in this assay are listed in Table S8.

Artificial selection test

To test whether there are artificial selections of *OsCLV2a*, *OsCLV2c*, *OsCLV2d*, and *OsCRN1*, we obtained the genetic variations in the 200-kb region around these genes in the RiceVarMap v2.0 database (including 3216 rice samples), and converted them into variant call format (VCF) files, and then analyzed its nucleotide diversity using VCFtools (0.1.16).

Accession numbers

Sequence data in this study were obtained from the Rice Genome Annotation Project website (MSU) and TAIR library with the following accession numbers: *OsCLV2a*, *LOC_Os02g39100*; *OsCLV2c*, *LOC_Os06g38930*; *OsCLV2d*, *LOC_Os06g38970*; *OsCLV2f*, *LOC_Os04g52780*; *OsCRN1*, *LOC_Os01g70260*.

CRediT authorship contribution statement

Xingxing Li: Data curation, Formal analysis, Investigation, Methodology, Resources, Writing − Original draft, Writing − Review & Editing. **Meng-en Wu:** Data curation, Formal analysis, Investigation, Resources, Writing − Original draft. **Juncheng Zhang:** Data curation. **Jingyue Xu:** Data curation. **Yuanfei Diao:** Data curation. **Yibo Li:** Conceptualization, Funding acquisition, Project administration, Supervision, Writing − Original draft, Writing − Review & Editing.

Conflict of interest

All authors declare no conflict of interest.

Acknowledgments

This study is supported by grants from STI 2030−Major Projects (2023ZD0406902), the National Key Research and Development Program of China (2022YFD1200103, 2023ZD04073), the National Natural Science Foundation of China (U22A20470, 32072042, 31821005), Hubei Hongshan Laboratory (2022hszd025, 2021hszd005), the Key Research and Development Program of Hubei (2023BBB135, 2022BBA0033) and the Fundamental Research Funds for the Central Universities (2662023PY002). We thank Prof. Jianmin Zhou (Chinese Academy of Sciences) for providing nLUC and cLUC vectors. We thank Prof. Ping Yin from Huazhong Agricultural University for kindly providing the prokaryotic expression vector of 28a-HIS-SUMO. We thank Waseem Abbas for drawing the working model.

Supplementary data

Supplementary data to this article can be found online at https://doi.org/10.1016/j.jgg.2024.03.011.

References

Bleckmann, A., Weidtkamp-Peters, S., Seidel, C., Simon, R., 2010. Stem cell signaling in Arabidopsis requires CRN to localize CLV2 to the plasma membrane. Plant Physiol. 152, 166−176.

Bommert, P., Lunde, C., Nardmann, J., Vollbrecht, E., Running, M., Jackson, D., Hake, S., Werr, W., 2005. *Thick tassel dwarf1* encodes a putative maize ortholog of the Arabidopsis *CLAVATA1* leucine-rich repeat receptor-like kinase. Development 132, 1235−1245.

Bommert, P., Nagasawa, N., Jackson, D., 2013. Quantitative variation in maize kernel row number is controlled by the *FASCIATED EAR2* locus. Nat. Genet. 45, 334−337.

Chen, H., Zou, Y., Shang, Y., Lin, H., Wang, Y., Cai, R., Tang, X., Zhou, J., 2008. Firefly luciferase complementation imaging assay for protein-protein interactions in plants. Plant Physiol. 146, 368−376.

Fan, Y., Li, Y., 2019. Molecular, cellular and Yin-Yang regulation of grain size and number in rice. Mol. Breed. 39, 163−188.

Fleming, A., 2015. Sweet size control in tomato. Nat. Genet. 47, 698−699.

Fletcher, J., 2018. The CLV-WUS stem cell signaling pathway: a roadmap to crop yield optimization. Plants 7, 87.

Gao, Y., Zhao, Y., 2014. Self-processing of ribozyme-flanked RNAs into guide RNAs in vitro and in vivo for CRISPR-mediated genome editing. J. Integr. Plant Biol. 56, 343−349.

Gupta, P., Kulwal, P., Jaiswal, V., 2019. Association mapping in plants in the post-GWAS genomics era. Adv. Genet. 104, 75–154.
Hanks, S., Quinn, A., Hunter, T., 1988. The protein kinase family: conserved features and deduced phylogeny of the catalytic domains. Science 241, 42–52.
Harberd, N., 2015. Shaping taste: the molecular discovery of rice genes improving grain size, shape and quality. J. Genet. Genomics 42, 597–599.
Hong, L., Fletcher, J., 2023. Stem cells: engines of plant growth and development. Int. J. Mol. Sci. 24, 14889.
Hu, C., Zhu, Y., Cui, Y., Cheng, K., Liang, W., Wei, Z., Zhu, M., Yin, H., Zeng, L., Xiao, Y., et al., 2018. A group of receptor kinases are essential for CLAVATA signalling to maintain stem cell homeostasis. Nat. Plants 4, 205–211.
Je, B., Gruel, J., Lee, Y.K., Bommert, P., Arevalo, E.D., Eveland, A.L., Wu, Q., Goldshmidt, A., Meeley, R., Bartlett, M., et al., 2016. Signaling from maize organ primordia via FASCIATED EAR3 regulates stem cell proliferation and yield traits. Nat. Genet. 48, 785–791.
Je, B., Xu, F., Wu, Q., Liu, L., Meeley, R., Gallagher, J., Corcilius, L., Payne, R., Bartlett, M., Jackson, D., 2018. The CLAVATA receptor FASCIATED EAR2 responds to distinct CLE peptides by signaling through two downstream effectors. Elife 7, e35673.
Jones, D., John, A., VanDerMolen, K., Nimchuk, Z., 2021. CLAVATA signaling ensures reproductive development in plants across thermal environments. Curr. Biol. 31, 220–227.
Kitagawa, M., Jackson, D., 2019. Control of meristem size. Annu. Rev. Plant Biol. 70, 269–291.
Li, N., Xu, R., Li, Y., 2019. Molecular networks of seed size control in plants. Annu. Rev. Plant Biol. 70, 435–463.
Li, T., Yang, X., Yu, Y., Si, X., Zhai, X., Zhang, H., Dong, W., Gao, C., Xu, C., 2018. Domestication of wild tomato is accelerated by genome editing. Nat. Biotechnol. 36, 1160–1163.
Lippert, C., Listgarten, J., Liu, Y., Kadie, C., Davidson, R., Heckerman, D., 2011. FaST linear mixed models for genome-wide association studies. Nat. Methods 8, 833–835.
Liu, Q., Feng, Z., Huang, C., Wen, J., Li, L., Yu, S., 2022. Insights into the genomic regions and candidate genes of senescence-related traits in upland cotton via GWAS. Int. J. Mol. Sci. 23, 8584.
Liu, Y., Wang, H., Jiang, Z., Wang, W., Xu, R., Wang, Q., Zhang, Z., Li, A., Liang, Y., Ou, S., et al., 2021a. Genomic basis of geographical adaptation to soil nitrogen in rice. Nature 590, 600–605.
Liu, L., Gallagher, J., Arevalo, E., Chen, R., Skopelitis, T., Wu, Q., Bartlett, M., Jackson, D., 2021b. Enhancing grain-yield-related traits by CRISPR-Cas9 promoter editing of maize *CLE* genes. Nat. Plants 7, 287–294.
Meng, L., Feldman, L., 2010. CLE14/CLE20 peptides may interact with CLAVATA2/CORYNE receptor-like kinases to irreversibly inhibit cell division in the root meristem of Arabidopsis. Planta 232, 1061–1074.
Müller, R., Bleckmann, A., Simon, R., 2008. The receptor kinase CORYNE of Arabidopsis transmits the stem cell-limiting signal CLAVATA3 independently of CLAVATA1. Plant Cell 20, 934–946.
Nimchuk, Z., 2017. CLAVATA1 controls distinct signaling outputs that buffer shoot stem cell proliferation through a two-step transcriptional compensation loop. PLoS Genet. 13, e1006681.
Purcell, S., Neale, B., Todd-Brown, K., Thomas, L., Ferreira, M., Bender, D., Maller, J., Sklar, P., de Bakker, P., Daly, M.J., et al., 2007. PLINK: a tool set for whole-genome association and population-based linkage analyses. Am. J. Hum. Genet. 81, 559–575.
Purugganan, M., Jackson, S., 2021. Advancing crop genomics from lab to field. Nat. Genet. 53, 595–601.
Rodríguez-Leal, D., Lemmon, Z., Man, J., Bartlett, M., Lippman, Z., 2017. Engineering quantitative trait variation for crop improvement by genome editing. Cell 171, 470–480.
Shinohara, H., Matsubayashi, Y., 2015. Reevaluation of the CLV3-receptor interaction in the shoot apical meristem: dissection of the CLV3 signaling pathway from a direct ligand-binding point of view. Plant J. 82, 328–336.
Somssich, M., Je, B., Simon, R., Jackson, D., 2016a. CLAVATA-WUSCHEL signaling in the shoot meristem. Development 143, 3238–3248.
Somssich, M., Bleckmann, A., Simon, R., 2016b. Shared and distinct functions of the pseudokinase CORYNE (CRN) in shoot and root stem cell maintenance of Arabidopsis. J. Exp. Bot. 67, 4901–4915.
Somssich, M., Ma, Q., Weidtkamp-Peters, S., Stahl, Y., Felekyan, S., Bleckmann, A., Seidel, C., Simon, R., 2015. Real-time dynamics of peptide ligand-dependent receptor complex formation in planta. Sci. Signal. 8, ra76.
Song, Y., Yang, H., Zhu, W., Wang, H., Zhang, J., Li, Y., 2023. The *Os14-3-3* family genes regulate grain size in rice. J. Genet. Genomics 51, 454–457.
Wang, C., Yu, H., Huang, J., Wang, W., Faruquee, M., Zhang, F., Zhao, X., Fu, B., Chen, K., Zhang, H., et al., 2020. Towards a deeper haplotype mining of complex traits in rice with RFGB v2.0. Plant Biotechnol. J. 18, 14–16.
Tao, Y., Zhao, X., Wang, X., Hathorn, A., Hunt, C., Cruickshank, A.W., van Oosterom, E.J., Godwin, L.D., Mace, E.S., Jordan, D.R., et al., 2020. Large-scale GWAS in sorghum reveals common genetic control of grain size among cereals. Plant Biotechnol. J. 18, 1093–1105.
Wang, W., Hu, C., Li, X., Zhu, Y., Tao, L., Cui, Y., Deng, D., Fan, X., Zhang, H., Li, J., et al., 2022. Receptor-like cytoplasmic kinases PBL34/35/36 are required for CLE peptide-mediated signaling to maintain shoot apical meristem and root apical meristem homeostasis in Arabidopsis. Plant Cell 34, 1289–1307.
Xu, C., Liberatore, K., MacAlister, C., Huang, Z., Chu, Y., Jiang, K., Brooks, C., Ogawa-Ohnishi, M., Xiong, G., Pauly, M., et al., 2015. A cascade of arabinosyltransferases controls shoot meristem size in tomato. Nat. Genet. 47, 784–792.
Ying, J., Gao, J., Shan, J., Zhu, M., Shi, M., Lin, H., 2012. Dissecting the genetic basis of extremely large grain shape in rice cultivar 'JZ1560'. J. Genet. Genomics. 39, 325–333.
Yu, S., Ali, J., Zhou, S., Ren, G., Xie, H., Xu, J., Yu, X., Zhou, F., Peng, S., Ma, L., et al., 2022. From Green Super Rice to green agriculture: reaping the promise of functional genomics research. Mol. Plant 15, 9–26.
Zhang, J., Zhang, D., Fan, Y., Li, C., Xu, P., Li, W., Sun, Q., Huang, X., Zhang, C., Wu, L., et al., 2021. The identification of grain size genes by RapMap reveals directional selection during rice domestication. Nat. Commun. 12, 5673.
Zhang, Q., 2007. Strategies for developing green super rice. Proc. Natl. Acad. Sci. U. S. A. 104, 16402–16409.
Zhao, H., Li, J., Yang, L., Qin, G., Xia, C., Xu, X., Su, Y., Liu, Y., Ming, L., Chen, L., et al., 2021. An inferred functional impact map of genetic variants in rice. Mol. Plant 14, 1584–1599.
Zhao, H., Yao, W., Ouyang, Y., Yang, W., Wang, G., Lian, X., Xing, Y., Chen, L., Xie, W., 2015. RiceVarMap: a comprehensive database of rice genomic variations. Nucleic Acids Res. 43, D1018–D1022.
Zhu, Y., Wang, Y., Li, R., Song, X., Wang, Q., Huang, S., Jin, J., Liu, C., Lin, J., 2010. Analysis of interactions among the CLAVATA3 receptors reveals a direct interaction between CLAVATA2 and CORYNE in Arabidopsis. Plant J. 61, 223–233.
Zsögön, A., Čermák, T., Naves, E., Notini, M., Edel, K., Weinl, S., Freschi, L., Voytas, D., Kudla, J., Peres, L., 2018. De novo domestication of wild tomato using genome editing. Nat. Biotechnol. 36, 1211–1216.
Zuo, J., Li, J., 2014. Molecular genetic dissection of quantitative trait loci regulating rice grain size. Annu. Rev. Genet. 48, 99–118.